Digital In-line Holographic PIV for 3D Flow Measurement

Gang Pan and Hui Meng
Department of Mechanical and Aerospace Engineering
State University of New York at Buffalo, Buffalo, NY 14260, USA

Abstract

We present the design and implementation of a digital in-line holographic PIV system for 3D flow measurements. This system records in-line holograms of tracer particles directly on a CCD camera and numerically reconstructs the holograms. The 3D position of particles is extracted from the reconstructed particle images, and velocity field is then obtained using an advanced particle tracking algorithm. With a novel complex amplitude-based method for particle extraction, we are able to overcome the depth of focus problem and the speckle noise problem which are intrinsic in digital particle holography. The system was tested in a laminar jet experiment. Instantaneous 3D flow field was successfully measured using this system.

Keywords: Holographic PIV, PIV, holography, digital holography

1. Introduction

Particle image velocimetry (PIV) has become a widely used technique for velocity measurement in many applications involving fluid flow. But conventional PIV systems can only provide two-dimensional (2D) velocity vectors in a single plane, which is often insufficient for answering many challenging questions in fluid dynamics concern complex three-dimensional (3D) flow. Efforts have been put on extending the spatial range of PIV technique to the third dimension. Among various extensions of 2D PIV, stereoscopic PIV is the most noticeable and commercial systems based on Scheimpflug configuration [1] have been developed. However, stereoscopic PIV is still based on lens imaging and hence it is confined to planar measurements. Recently systems using scanning or multiple laser sheets have been implemented to extend stereoscopic PIV to multiple plane measurements [2, 3], but these systems suffers from extreme complexity or lack of temporal resolution to be practical in many applications. Defocusing digital particle image velocimetry (DDPIV) [4] is another type of PIV technique that utilizes a unique defocusing optical setup to generate images with imbedded instantaneous information on the 3D spatial position of particles. DDPIV is capable of measuring instantaneous 3D velocity field in a

fairly large volume with a combined dynamic range, resolution and reliability. Unfortunately this technique is limited in particle number density.

Holographic PIV [5] has been praised for its high potential in instantaneous, volumetric and 3D measurement of flow velocity field. Unlike photography-based PIV systems, holographic PIV records the 3D information of tracer particles in a fluid *volume* instantaneously by capturing the phase information of light waves scattered off the particles, and then reconstructs the "frozen" particle images in a 3D space. From the reconstructed image field, one can retrieve the 3D positions of tracer particles. By finding the 3D displacements of the tracer particles in the image volume between two exposures separated by a very brief time lapse, the instantaneous 3D velocity field of the flow can be obtained.

The silver-halide-based holographic film, which offers a superior resolution (as high as 5000 line pairs per mm), is usually chosen to perform volumetric recording in holographic PIV. Unfortunately, the holographic films require chemical developing and fixing, a process increasingly viewed as undesirable by potential users. Furthermore, the optical reconstruction requires tedious mechanical scanning of the reconstructed image volume, a process that takes up most of the data processing time. As a result, most holographic PIV systems [6-9] are restricted to single-shot, and cinematic holographic PIV [10] to provide temporal measurements remains an unfulfilled promise.

To circumvent the drawbacks associated with film-based recording and optical reconstruction, digital holography has been recently explored as an alternative for 3D particle and flow measurement [11,12]. With the digital holographic approach, holograms are directly recorded on a digital camera and reconstructed numerically [13]. This not only eliminates wet chemical processing and mechanical scanning but also allows flexible reconstruction algorithms to achieve optimization of specific information. Furthermore, digital holography greatly simplifies the hardware setup for cinematic holographic recording and reconstruction, hence making cinematic implementation of holographic PIV much easier.

Despite these promising prospects, digital holography is inherently limited by the poor resolution of solid-state image sensors. Currently the smallest pixel size of scientific CCD sensors is around 4 μm, compared with the silver-halide holographic films with an equivalent pixel size down to 0.1 μm. Since the digital sensor elements cannot resolve interference fringes finer than the pixel size, the permissible angle between object wave and reference wave is limited to a few degrees. Consequently the numerical aperture (N. A.) of a digital hologram is often less than 0.1. In digital particle holography, a small numerical aperture leads to very large depth of focus in the reconstructed particle images. It may also result in excessive speckle noise when particle number

density is high. The depth of focus problem and the speckle noise problem severely restrict the practicality of digital holographic PIV, where accurate particle 3D positions and high particle number density are essential for high-resolution accurate velocity measurement.

In this paper we present the design and implementation of our digital in-line holographic PIV system. We first describe the digital recording setup and the numerical reconstruction procedure. Then we introduce how we overcome the aforementioned problems by using a novel particle extraction method which is based on complex amplitude of the reconstruction wave [14]. The velocity extraction using the particle matching algorithm [15] is also described. Finally we present the testing result of a laminar jet experiment.

2. Digital Holographic PIV System

Figure 1 shows the optical setup for hologram recording in our digital holographic PIV system. To minimize spatial resolution requirement in hologram recording, in-line holography is adopted, where the unscattered part of the illumination wave serves as the reference wave to interfere with the wave scattered by the particles. The 514-nm coherent light from an Argon laser (Coherent Innova 90) is used for hologram recording. To enable two-frame, double-exposure PIV, the laser beam is modulated by an acousto-optic Bragg cell (IntraAction AOM 404-A1) to generate a pair of briefly separated light pulses at a given frequency. The pulsed laser beam is then collimated to form a plane illumination wave for in-line holographic recording. The illumination area is shaped by a square aperture of 1 cm × 1 cm to fit the size of image sensor. Digital holograms are recorded by a 12-bit CCD camera with the active area measuring 8.6 × 6.9 mm^2 (PCO SensiCam, 12 bit, 1280 × 1024 pixels, pixel size 6.7 μm × 6.7 μm). To ensure proper timing in the experiment, the Bragg cell and the CCD camera are synchronized by an internal timing board (Keithely CTM-10) and an external pulse generator (BNC model 555).

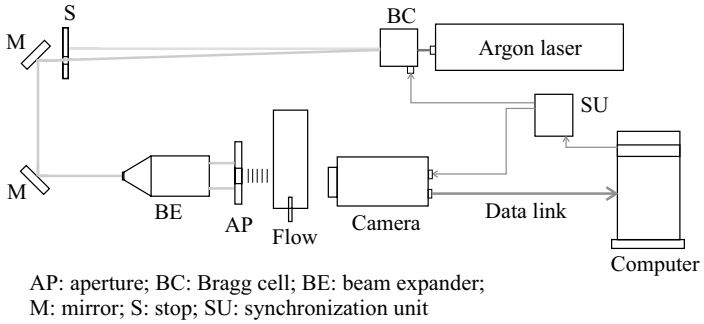

Fig. 1. Optical setup for hologram recording.

Figure 2 illustrates the flow chart in data processing. The first step is hologram preprocessing to correct inhomogeneous illumination and to remove background noise. Then the digital

holograms are numerically reconstructed to obtain the total reconstruction wave in the image volume. The 3D coordinates of tracer particles are extracted from the total reconstruction wave using a complex amplitude-based method. Two sets of particles are retrieved from two briefly spaced exposures respectively. Finally the 3D velocity field is obtained by using a particle tracking algorithm that works with the coordinates of particle centroid.

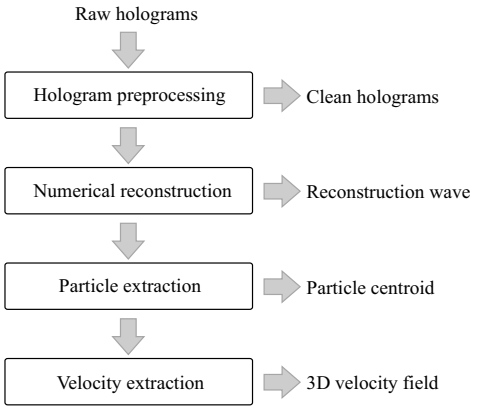

Fig. 2. Data flow chart for hologram processing.

2.1 Digital hologram recording

Solid-state image sensor such as CCD or CMOS image sensor consists of a matrix of neighboring photodiodes called pixels. The voltage readout of each pixel is proportional to the *average* light intensity in that pixel. Therefore, in digital holography a hologram is essentially the discrete sampling of a continuous, *low-pass filtered* intensity function. Denoting Δ as the pixel size and N as the number of pixels of a CCD sensor, the discrete intensity function I_H (the hologram) can be written as

$$I_H(m,n)=\left\{I_w(\xi,\eta)\otimes\left[rect(\xi/\Delta)\cdot rect(\eta/\Delta)\right]\right\}\times\delta\left[\xi-(m-1/2)\Delta,\eta-(n-1/2)\Delta\right] \quad (1)$$

where m and n are pixel index from 1 to N; I_w is the original intensity functions; *rect* is the rectangular box function, and $\otimes$ denotes the convolution.

According to the sampling theorem, the Nyquest wave number of a CCD sensor is π/Δ. This resolution is insufficient to fully resolve the spectrum of a hologram even in in-line holography. However, as defined in Eq. (1), the discrete sampling is actually performed with the *low-pass filtered* intensity function instead of the original intensity function I_w. Due to the convolution with the rectangular box function, the bandwidth of the *low-pass filtered* intensity function is limited to $2\pi/\Delta$. As a result, although the recording resolution is low, the aliasing error caused by under-sampling is minor in digital holograms.

2.2 Numerical Hologram Reconstruction

2.2.1 Hologram preprocessing

With traditional holography, holograms cannot be bettered once they are recorded and developed. Hence the hologram reconstruction has to tolerate any imperfection in hologram recording. This drawback can be overcome in digital holography since various imaging processing techniques can be applied on digital holograms to achieve the optimization of the reconstruction images. For example, the fringe contrast of a hologram can be improved by image equalization; the inhomogeneous illumination in recording can be corrected by background subtraction; and the noise fringes caused by dirt or other objects along the optical path can be eliminated through appropriate filtering operation. Shown in Fig. 3 are the holograms after subsequent preprocessing steps. The left picture is the raw hologram, which suffers from inhomogeneous illumination and prominent background fringes; the middle one is the hologram processed by local-mean subtraction (LMS) filter, which removes the effect of inhomogeneous illumination; and the right one is the hologram after both LMS filtering and the spectrum-selection (SS) filtering, which is the clean hologram we will use for reconstruction. Details of the LMS filter and SS filter are given below.

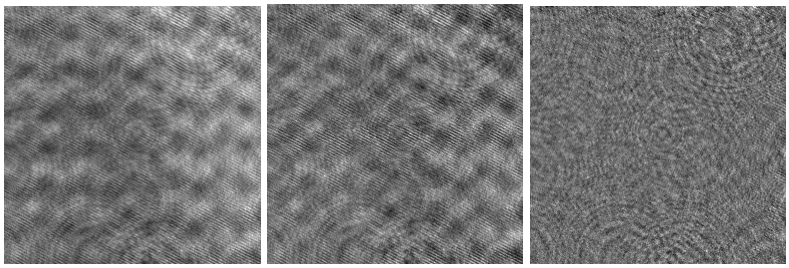

Fig. 3. Digital holograms after subsequent preprocessing steps.

(a) **Local-mean subtraction filter**: With this filter, the gray level at each pixel is subtracted by the local average in a small square window. The filter is defined in the wave number domain,

$$I_{H,lms}(u,v) = I_H(u,v) \cdot \left[1 - \mathrm{sinc}(W \cdot u) \cdot \mathrm{sinc}(W \cdot v)\right] \qquad (2)$$

where W is the size of the averaging window. The local-mean subtraction filter is essentially a high-pass filter, and therefore it can also remove the *dc* component in hologram reconstruction.

(b) **Spectrum-selection filter**: The apparent background fringes in the raw holograms are caused by the beam expander and the cover glass in front of the CCD sensor. The regular pattern of these fringes results in a few particularly strong wave-number components in the power spectrum of the holograms. Therefore, a spectrum-selection filter is designed to detect those wave-number components through the power spectrum and then change their Fourier coefficient to zero.

2.2.2 Numerical reconstruction

Conventionally, the optical reconstruction is performed by placing the holograms back into the recording setup and illuminating by the same coherent reference wave. The diffraction of the reference wave by the hologram yields the total reconstruction wave consisting of four terms:

$$U = |R|^2 + |O|^2 + R^* O + R O^*, \qquad (3)$$

where $\boldsymbol{R}$ is the reference wave, $\boldsymbol{O}$ is the object wave, $\boldsymbol{R}^*\boldsymbol{O}$ is the virtual image wave and $\boldsymbol{R}\boldsymbol{O}^*$ is the real image wave.

In digital holography, hologram reconstruction can be performed numerically by applying the scalar diffraction theory. A simple model for reconstruction in digital holography is outlined in Fig. 4. The hologram $I_H(\xi, \eta)$ is located at the plane $z = 0$, and the reconstruction wave $\boldsymbol{U}(x, y)$ at any transverse plane is given by Rayleigh-Sommerfelds diffraction formula,

$$U(x, y, z) = \frac{1}{j\lambda} \iint I_H(\xi, \eta) R(\xi, \eta) \frac{\exp(jkr)}{r} \cos\Theta d\xi d\eta \qquad (4)$$

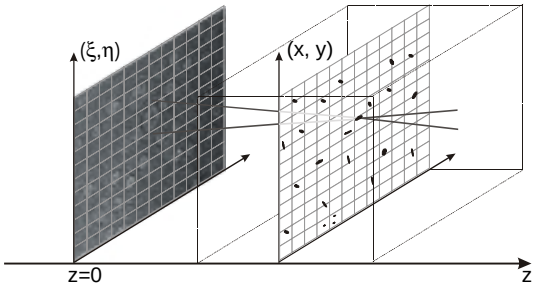

Fig. 4. Coordinate system in hologram reconstruction.

where $\boldsymbol{R}(\xi, \eta)$ is the illumination wave in hologram reconstruction. r is the distance from point $(\xi, \eta, 0)$ in the hologram plane to point (x, y, z) in the reconstruction plane. $\cos\Theta$ is the obliquity factor that can be approximated by $\cos\Theta \cong 1$ where the accuracy is to within 5% if the angle Θ does not exceed 18°. Accepting the validity of the Fresnel approximation, the diffraction integral in Eq. (4) becomes

$$U(x, y, z) = \iint I_H(\xi, \eta) R(\xi, \eta) \frac{\exp(jkz)}{j\lambda z} \exp\left\{\frac{jk}{2z}\left[(x-\xi)^2 + (y-\eta)^2\right]\right\} d\xi d\eta \qquad (5)$$

where the total reconstruction wave may be regarded as a convolution of $I_H R$ with the kernel function h, which is given explicitly by

$$h_z(x, y) = \frac{1}{j\lambda z} \exp\left\{\frac{jk}{2z}\left(x^2 + y^2\right)\right\} \qquad (6)$$

Applying the convolution theorem, the numerical implementation of the diffraction integral in Eq. (5) can be carried out efficiently by using Fast Fourier Transform (FFT).

To reconstruct the 3D objects recorded by a hologram, the total reconstruction wave $\boldsymbol{U}$ in a series of transverse planes is computed. The intensity distribution in each reconstruction plane is equivalent to the photographic image focusing at that particular plane. This reconstruction scheme is the numerical simulation of the mechanical scanning that is often used in optical reconstruction.

2.3 Extraction of particle information

Since the velocity field is obtained from the displacement of tracer particles in two briefly spaced exposures, it is crucial to develop a robust and accurate method for extracting particle position from the reconstructed 3D image field. In optical reconstruction particle extraction is solely based on the intensity information since sensors used for interrogating the reconstructed image field only respond to light intensity. With numerical reconstruction, however, the complex amplitude of the reconstruction wave is obtained in numerical form and thereby both intensity and phase data are immediately available. This unique feature of numerical reconstruction extends particle extraction to the complex number domain and thereby facilitates new solution to the depth of focus problem and the speckle noise problem which are intrinsic in particle holography.

2.3.1 Particle 3D images

In hologram reconstruction, particle 3D images are obtained from the intensity of the total reconstruction wave $\boldsymbol{U}$. Firstly the 2D objects are found in each scanning plane using image processing tools such as thresholding, boundary tracing, and object labeling. Then particle 3D images are constructed by clustering the overlapped 2D objects on adjacent planes in the transverse direction.

Due to the small aperture of digital holograms, the reconstructed particle 3D images have remarkably large depth of focus. Simulation results have shown that the depth of focus of particle intensity images is more than 40 times of particle diameter. Such a large depth of focus severely restricts the depth resolution of intensity-based particle extraction and compromises the 3D imaging capability of digital holography.

2.3.2 PECA method

Based on digital recording and numerical reconstruction, we have developed a novel method for particle extraction using complex amplitude (PECA). This method uses the complex amplitude of the total reconstruction wave to extract particle depth position. Particle transverse positions are then obtained directly from the intensity image at the particle in-focus plane.

It was found that, in the reconstruction of particle holograms formed by forward scattering, the imaginary part of the object wave vanishes at the in-focus plane of the particles. As a result, the variance of the imaginary part of $\boldsymbol{U}$, which is defined in a transverse plane for the pixels belonging to the 2D image of a particle, is the minimum at the in-focus plane of that particle. This so-called dipping characteristic of the total reconstruction wave is demonstrated in Fig. 5, where the variance of $Im(\boldsymbol{U})$ in the planes near a particle is plotted against the planes' out-of-focus distance. The curve displays the dipping shape with its minimum at the in-focus position of $z = z_p$.

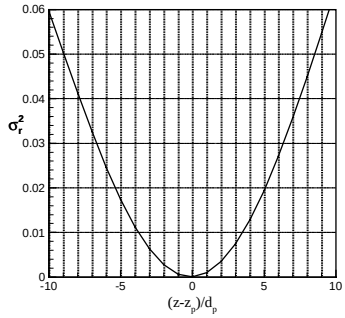

Fig. 5. The dipping characteristic of Im(*U*).

By virtue of the dipping characteristic the PECA method can achieve very high accuracy in extracting particle depth positions regardless of the small numerical aperture of digital holograms. Fig. 6 shows the calibration result using synthesized holograms with particle number density of 18 particle/mm^3. The particle depth positions obtained by the PECA method and the conventional intensity method were compared with the known position of the particles, and the cumulative distribution functions of the error of depth position δ_z were calculated. With PECA method, δ_z is less than 20 μm for more than 80% of the extracted particles, while with the intensity method that percentage is less than 30%. More detailed description of the PECA method can be found in Pan and Meng [14].

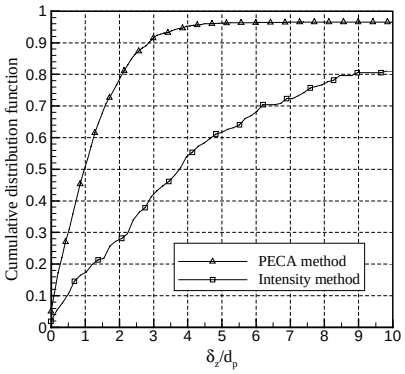

Fig. 6. Depth error of two particle extraction methods.

2.3.3 Speckle noise

Speckle noise problem is intrinsic in particle holography especially in holographic PIV due to the dense particle distribution in the sample volume. It was found that, in the reconstruction of particle holograms, the speckle noise level increases proportionally with particle number density and sample volume depth [16]. Moreover, the characteristic speckle size is comparable with the particle image size no matter how much the recording resolution is. This makes particle recognition extremely difficult in densely populated particle fields where the intensity level of speckle noise could be comparable with the intensity of particle images. Consequently, a lot of "false particles" are generated in particle extraction, which will prohibit any meaningful velocity extraction.

To overcome the speckle noise problem, we have implemented an effective method in our system by virtue of the flexible numerical reconstruction scheme and the dipping characteristic of the reconstruction wave. This method consists of two steps: (a) suppressing speckle noise in hologram reconstruction and (b) detecting speckles in particle extraction.

(a) **Suppressing speckle noise**: In reconstruction of in-line particle holograms, the real image wave of out-of-focus particles and the virtual image wave are two major sources of speckle noise. For far-field particle holography, the magnitude of virtual image wave is very weak in the region where particles are extracted. Therefore, the contribution of virtual image wave to the speckle noise can be effectively suppressed if the directed transmitted wave is not presented in the reconstruction so that the interference between the two waves is avoided. In numerical reconstruction the directed transmitted wave is the *dc* term in the Fourier domain and hence it can be easily filtered. As a result, the speckle noise level is decreased shapely and the real image wave of out-of-focus particles becomes the dominant source of the speckle noise.

(b) **Detecting speckles**: Due to their comparable size and intensity level, speckles and particles cannot be differentiated in the intensity images. But detecting speckles is possible in the complex amplitude domain. We know that speckles are formed by the summation of the real image wave of out-of-focus particles. This summation can be viewed as a random walk process in the complex plane, which does not produce the dipping pattern of the complex amplitude of $\boldsymbol{U}$. Therefore the dipping shape of the variance of $Im(\boldsymbol{U})$ can be used to distinguish speckles from particles.

2.4 Extraction of velocity field

In digital HPIV, velocity extraction is very difficult due to the relatively low seeding densities and a large number of unpaired particles resulting from speckle noise and particle position errors. In our system we choose the particle tracking approach for velocity extraction. The particle

matching (PM) algorithm, originally developed by Stellmacher and Obermayer [15], was adopted to extract 3D velocity of individual particles from their coordinate in subsequent exposures.

After the coordinates of particles have been extracted using the PECA method, the sample volume is divided into a number of 3D interrogation cells (IC). For each IC, the input data to the PM algorithm consists of two lists $\{X_j\}$ and $\{Y_k\}$ of particle 3D coordinates, where x_j is for the first frame and y_k the second. The correspondences between particles j in the first frame and particle k in the second are described by the binary correspondence matrix $M = \{m_{kj}\}$, where m_{kj} = 1 if particle j corresponds to particle k and $m_{kj} = 0$ otherwise. A transformation function $T(\pi)$, where π denotes a set of flow field parameters, is defined for each IC to describe the movement of particles between the two frames. The estimation of the correspondence matrix M provides the velocity vector for every particle pair. Transformation parameters π, on the other hand, provide the local velocity, rotation, or shear components for the whole IC.

To get the optimal estimation of M and π, the PM algorithm defines a cost function $E(M, \pi)$ which measures the goodness of every hypothesis about the correspondences M between particles and the parameters π of the local flow field. $E(M, \pi)$ is then minimized using the expectation-maximization (EM) algorithm in combination with the deterministic annealing scheme. The EM algorithm consists of an expectation step (E-step) and a maximization step (M-step). In the E-step, the correspondence matrix M is calculated using particle coordinates $\{X_j\}$ and $\{Y_k\}$ and the parameters π of the local flow field. In the M-step, the estimation of local flow field is updated using the new correspondence matrix. The E-step and the M-step are repeated until the difference of $E(M, \pi)$ is very small. The whole EM algorithm is enclosed by an outer loop which implements the deterministic annealing to assure that binary values are obtained in the correspondence matrix M.

Contrary to conventional correlation-based methods in PIV, the PM algorithm extracts not only translation but also rotation and shear component of the velocity, which makes it superior to other methods in regions with high velocity gradients. Moreover, the estimation of local flow parameters and particle correspondences are performed simultaneously: particle correspondences help to calculate flow-field parameters which, in turn, help to disambiguate particle correspondence. This makes the PM algorithm robust against low seeding densities and missing particles.

3. Testing Experiment

The digital in-line holographic PIV system was tested in a water jet experiment. The schematic of the experimental setup is shown in Fig. 7. The gravity-driven flow issued from a vertical tube (1.4 mm ID, stainless steel) forms the jet in the middle of a glass tank (50 mm width, 10 mm depth, and 50 mm height). A small reservoir is put on top of the glass tank to avoid free-surface effect in the near field of the jet. The Reynolds number based on jet exit velocity and jet diameter is about 140.

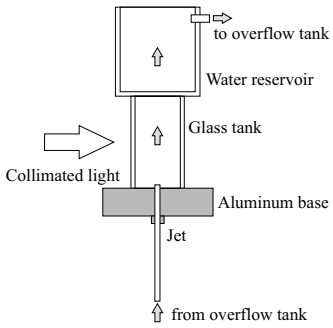

Fig. 7. Experimental setup for the laminar jet flow.

During the experiment, the distilled water is seeded with neutrally buoyant, mono-disperse particles (7 μm diameter, Duke Scientific 2007A) at a seeding density of about 12 particle/mm^3. The sample volume measures 8.6 × 6.9 × 10 mm^3 and the volume thickness is 10 mm. Two-frame, double-exposure holograms of tracer particles are recorded at 4 frame pairs per second by a 12-bit CCD camera. The time interval between subsequent exposures is 20 ms and each exposure lasts 5 μs.

The holograms were numerically reconstructed to obtain the double-exposure image of the tracer particles. Shown in Fig. 8 is an example of the reconstructed image (double exposure) of a 1.3 mm^3 cube. The image quality is superior to that in optical in-line holography because the twin-image effect is effectively suppressed by filtering the *dc* component in numerical hologram reconstruction.

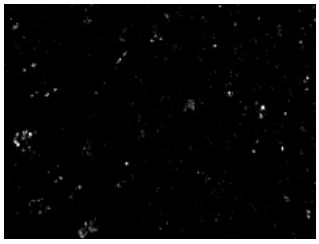

Fig. 8. A portion of the reconstructed double-exposure HPIV image.

From the reconstruction wave field we first extracted the 3D coordinate of particles using the PECA method. Then we used the PM algorithm to track individual particles and obtain their 3D

velocity. Finally the instantaneous 3D velocity field was obtained by interpolating the velocity of particles onto a structured grid (using the Gaussian interpolation scheme). Shown in Fig. 9 is the 3D velocity vector map on three perpendicular planes which are extracted from the 3D sample volume. The jet enters the sample volume at the center in the bottom plane and moves upward along the Y-axis. The jet-induced flow is clearly seen from the velocity vector map. The streamlines, shown in Fig. 10, were also obtained from the 3D velocity field.

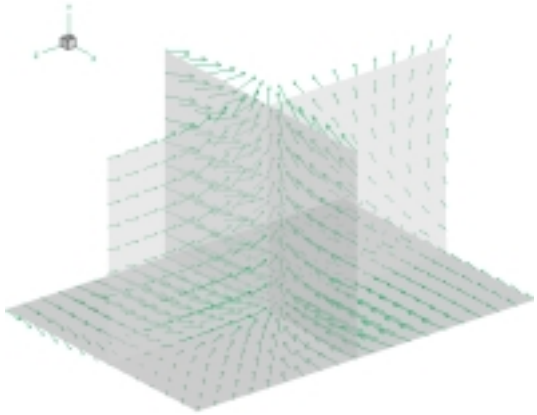

Fig. 9. Digital HPIV measurement of 3D velocity field near the exit of a water jet.

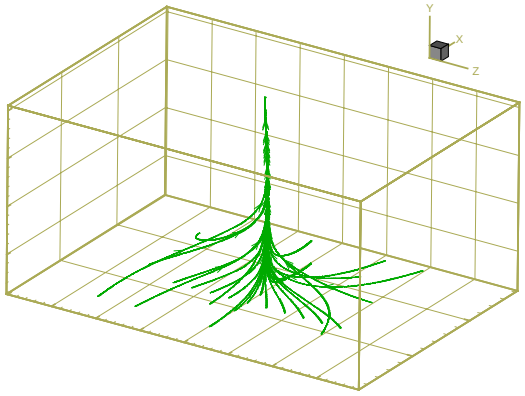

Fig. 10. Streamlines in the near field of the water jet.

4. Summary

We have developed a digital in-line holographic PIV system for 3D flow measurement. This system records in-line holograms of tracer particles directly on a digital camera and numerically reconstructs the holograms. The Fresnel approximation of the Rayleigh-Sommerfelds diffraction formula is used for numerical reconstruction. To improve the quality of reconstruction images, background noise and inhomogeneous illumination are removed from the digital holograms prior to the hologram reconstruction. A novel complex amplitude-based method (PECA) has been developed for particle extraction from the reconstructed images [14]. The PECA method

significantly improves the depth resolution of particle extraction and can provide accurate results even for densely populated particle fields. The PECA method also enables speckle detection and thereby greatly alleviates the speckle noise problem which is intrinsic in particle holography. Velocity extraction is done by using the particle matching (PM) algorithm [15]. This algorithm uses the expectation-maximization algorithm to find the optimal estimation of particle matching and the local flow parameters simultaneously. It works very well with low seeding densities and is robust against missing particles. The digital in-line HPIV system has been tested in a laminar jet flow and instantaneous 3D velocity field is successfully measured.

References

1. Prasad, K., and Jensen, K., 1995, "Scheimpflug stereocamera for particle image velocimetry in liquid flows," Appl. Opt., **34**, pp. 7092-7099.
2. Bruecker, C., 1997, "3D scanning PIV applied to an air flow in a motored engine using digital high-speed video," Meas. Sci. Technol., **8**, pp. 1480-1492.
3. Kahler, C. J., and Kompenhans, J., 2000, "Fundamentals of multiple plane stereo particle image velocimetry", Exp. in Fluids, **29**, pp. S70-S77.
4. Pereira, F., and Gharib, M., 2002, "Defocusing digital particle image velocimetry and the three-dimensional characterization of two-phase flows," Meas. Sci. Technol., **13**, pp.683-694.
5. Hinsch, K. D., 2002, "Holographic particle image velocimetry," Meas. Sci. Technol., **13**, pp. R61-R72.
6. Barnhart, D. H., Adrian, R. J., Meinhart, C. D., Papen G. C., 1994, "Phase-conjugate holographic system for high-resolution particle image velocimetry," Appl. Opt., **33**, 7159-7169.
7. Meng, H, Hussain, F, 1995, "In-line Recording and Off-axis Viewing (IROV) technique for holographic particle velocimetry," Appl. Opt., **34**, pp.1827-1840.
8. Zhang, J, Tao, B, Katz, J, 1997, "Turbulent flow measurement in a square duct with hybrid holographic PIV," Exp. Fluids, **23**, pp.373-381.
9. Pu, Y., Meng, H., 2000, "An advanced off-axis holographic particle image velocimetry (HPIV) system," Exp. Fluids, **29**, 184-197.
10. Meng, H., Hussain, F., 1991, "Holographic particle velocimetry, a 3D measurement technique for vortex interactions, coherent structures and turbulence," Fluid Dynamics Research, **8**, 33-52.
11. Adams M., Kreis T., Juptner W., 1997, "Particle size and position measurement with digital holography," in Optical Inspection and Micromeasurements II, C. Gorecki, ed., Proc. SPIE **3098**, pp. 234-240
12. Owen, R. B., Zozylya, A. A., 2000, "In-line digital holographic sensor for monitoring and characterizing marine particulates," Opt. Eng., **39**, pp. 2187-2197.
13. Onural, L., Scott, P. D., 1987, "Digital decoding of in-line holograms," Opt. Eng., **26**, pp. 1124-1132.
14. Pan, G., and Meng, H., 2002, "Digital holography of particle fields: reconstruction using complex amplitude," to appear in Appl. Opt.

15. Stellmacher M., Obermayer K., 2000, “A new particle tracking algorithm based on deterministic annealing and alternative distance measures,” Exp. Fluids, 28, 506-518.
16. Meng, H., Anderson, W. L., Hussain, F., and Liu, D., 1993, “Intrinsic speckle noise in in-line particle holography,” J. Opt. Soc. of Am. A, 10, 2046-2058.